Comparison of Orthogonal Frequency-Division Multiplexing and On-Off Keying in Amplified Direct-Detection Single-Mode Fiber Systems

Daniel J. F. Barros and Joseph M. Kahn, *Fellow, IEEE*

***Abstract*—We discuss the use of orthogonal frequency-division multiplexing (OFDM) for combating group-velocity dispersion (GVD) effects in amplified direct-detection (DD) systems using single-mode fiber. We review known OFDM techniques, including asymmetrically clipped optical OFDM (ACO-OFDM), DC-clipped OFDM (DC-OFDM) and single-sideband OFDM (SSB-OFDM), and derive a linearized channel model for each technique. We present an iterative procedure to achieve optimum power allocation for each OFDM technique, since there is no closed-form solution for amplified DD systems. For each technique, we minimize the optical power required to transmit at a given bit rate and normalized GVD by iteratively adjusting the bias and optimizing the power allocation among the subcarriers. We verify that SSB-OFDM has the best optical power efficiency among the different OFDM techniques. We compare these OFDM techniques to on-off keying (OOK) with maximum-likelihood sequence detection (MLSD) and show that SSB-OFDM can achieve the same optical power efficiency as OOK with MLSD, but at the cost of requiring twice the electrical bandwidth and also a complex quadrature modulator. We compare the computational complexity of the different techniques and show that SSB-OFDM requires fewer operations per bit than OOK with MLSD.**

***Index Terms*—Communications system performance, direct-detection, group-velocity dispersion, intensity modulation, maximum-likelihood sequence detection, maximum-likelihood sequence estimation, multi-carrier optical systems, orthogonal frequency-division multiplexing.**

I. Introduction

RECEIVER-BASED electronic signal processing in optical communication systems has been the subject of many recent studies. In coherent systems, linear equalizers have been shown to fully compensate linear fiber impairments in single-mode fiber (SMF), such as group-velocity dispersion (GVD) and polarization-mode dispersion (PMD) [1]. On the other hand, in systems using direct-detection (DD), linear equalizers offer little performance improvement, because the nonlinear photodetection process destroys information on the phase of the received electric field. Recently, maximum-likelihood sequence detection (MLSD) was shown to be effective in mitigating GVD and PMD impairments in DD links [2], [3]. Although the computational complexity of MLSD increases exponentially with the channel memory, using low-complexity branch metrics, near-optimal performance can be achieved with manageable computational complexity, provided the effective channel memory does not exceed a few symbol intervals [4].

An alternate approach to combating fiber impairments in amplified DD systems is to use multicarrier modulation, such as orthogonal frequency-division multiplexing (OFDM). There are three major approaches for combining OFDM with DD. The first two techniques are based on intensity modulation (IM), and so require some means to make the OFDM signal nonnegative. The first technique adds a DC bias to reduce the negative signal excursions and then clips the remainder of the negative excursions. This method is called DC-OFDM. The second technique clips the entire negative excursion of the waveform, avoiding the need for a DC bias [5], [6]. Clipping noise is avoided by appropriate choice of the subcarrier frequencies. This technique is called asymmetrically clipped optical OFDM (ACO-OFDM). The third technique is based on single-sideband modulation of the complex-valued optical electric field by an OFDM signal. A DC bias (carrier component) is added, leaving a guard band between the carrier and the OFDM signal in order to avoid intermodulation products caused by photodetection [7], [8]. This method is called single-sideband OFDM (SSB-OFDM).

There have been several studies of the different OFDM techniques (e.g., [6]), but there has been no comparison of power efficiencies among the various direct-detection OFDM methods in SMF, and to conventional baseband methods, such as on-off keying (OOK). Furthermore, in previous work, the DC bias and the powers of the subcarriers were not jointly optimized based on the channel response and the nonlinear beat noises, since there is no closed-form solution for this optimization. We present an iterative procedure based on known bit-loading algorithms with a new modification, the bias ratio (BR), in order to obtain the optimum power allocation. We compare the performance of the three OFDM techniques using optimized power allocations to the performance of OOK with MLSD.

This paper is organized as follows. In Section II, we review methods for power and bit allocation for multicarrier systems and describe the optimal water-filling solution. We present our system model in Section III. In Section IV, we review the different OFDM formats and derive equivalent linear channel models for each one, assuming only GVD is present in the

Manuscript received January 29, 2010; revised April 15, 2010; accepted April 18, 2010. Date of publication April 29, 2010; date of current version June 02, 2010. This work was supported by the Portuguese Foundation for Science and Technology scholarship SFRH/BD/22547/2005 and by a Stanford Graduate Fellowship.

The authors are with the Department of Electrical Engineering, Stanford University, Stanford, CA 94305-9515 USA (e-mail: djbarros@stanford.edu; jmk@ee.stanford.edu).

Digital Object Identifier 10.1109/JLT.2010.2048999

SMF. Furthermore, we discuss the effects of amplifier noise in direct-detection systems and compute an expression for the autocorrelation function of the photodetected noise. In Section V, we compare the optical power required to transmit at a given bit rate for the different optimized OFDM formats and for OOK with MLSD, making use of previously published results for the latter format. In that section, we also compare the computational complexities of the various formats. We present conclusions in Section VI.

II. Power and Bit Allocation

A. Gap Approximation

On an AWGN channel, the maximum achievable bit rate is given by the Shannon capacity

$$\frac{C}{B} = \log_2(1 + \mathrm{SNR}), \tag{1}$$

where C is the capacity, B is the channel bandwidth and SNR is the signal-to-noise ratio. Any real system must transmit at a bit rate less than capacity. For QAM modulation, the achievable bit rate can be expressed approximately as

$$\frac{R}{B} = \log_2\left(1 + \frac{\mathrm{SNR}}{\Gamma}\right), \tag{2}$$

where R is the bit rate and Γ is called the gap constant. The gap constant, introduced by Cioffi *et al.* [9] and Forney *et al.* [10], represents a loss with respect to the Shannon capacity.

The gap analysis is widely used in the bit loading of OFDM systems, since it separates coding gain from power-allocation gain [11]. For uncoded QAM, the gap constant is given by

$$\Gamma = \frac{\alpha^2}{3}, \tag{3}$$

where $\alpha = Q^{-1}(P_e)$, P_e is the symbol-error probability and Q^{-1} is the inverse Q function. As an example, the gap is 8.8 dB at $P_e = 10^{-6}$ and is 9.5 dB at $P_e = 10^{-7}$ for uncoded QAM. The use of forward error-correction (FEC) codes reduces the gap. A well-coded system may have a gap as low as 0.5 dB at $P_e < 10^{-6}$. A gap of 0 dB means the maximum bit rate has been achieved and therefore $R = C$. Fig. 1 shows the attainable bit rates for various gap values.

For the remainder of the paper, we define the normalized bit rate $b = R/B$, which has units of bits/s/Hz.

B. Optimum Power Allocation

The OFDM signal splits the transmission channel into N parallel channels. When the total average transmitted power is constrained, the maximum obtainable bit rate can be written as

$$\max_{\mathrm{P_n}} \mathrm{b} = \sum_{n=0}^{N-1} \log_2\left(1 + \frac{P_n|H_n|^2}{\Gamma\sigma_n^2}\right)$$
$$\text{subject to } P_t = \sum_{n=0}^{N-1} P_n, \tag{4}$$

where $|H_n|^2, \sigma_n^2$ and P_n are the channel gain, noise variance and transmitted power at subcarrier n, respectively, and P_t is total average transmitted power. The solution of (4) is the known water-filling solution

$$P_n + \frac{\Gamma\sigma_n^2}{|H_n|^2} = a, \tag{5}$$

where a is a constant chosen such that $P_t = \sum_n P_n$. The optimum power allocation is then

$$P_n = \begin{cases} a - \dfrac{\Gamma\sigma_n^2}{|H_n|^2}, & a \geq \dfrac{\Gamma\sigma_n^2}{|H_n|^2} \\ 0, & a < \dfrac{\Gamma\sigma_n^2}{|H_n|^2} \end{cases}. \tag{6}$$

The optimum power allocation is illustrated in Fig. 2.

After the optimum power allocation is determined, the number of bits to be transmitted on each subcarrier is computed using (2). While the ideal value of $b = R/B$ is an arbitrary nonnegative real number, in practice, the constellation size and FEC code rate are adjusted to obtain a close rational approximation. In our analysis, we will neglect the difference between the ideal value of b and its rational approximation.

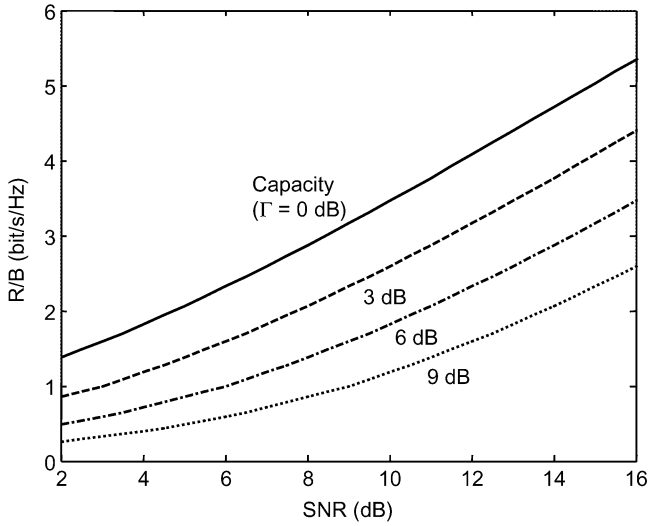

Fig. 1. Achievable bit rates as a function of SNR for various values of the gap Γ.

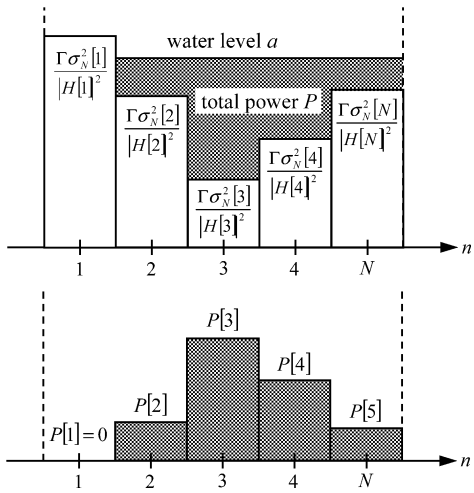

Fig. 2. Optimal power allocation for OFDM.

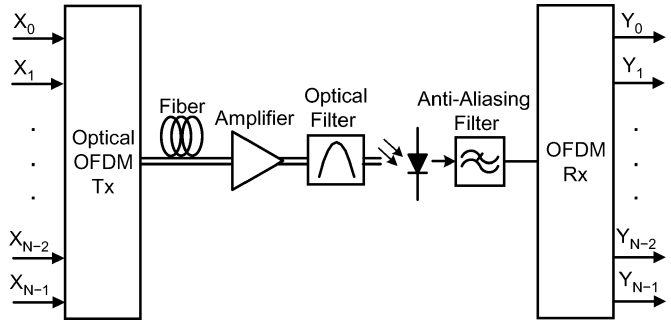

Fig. 3. System model.

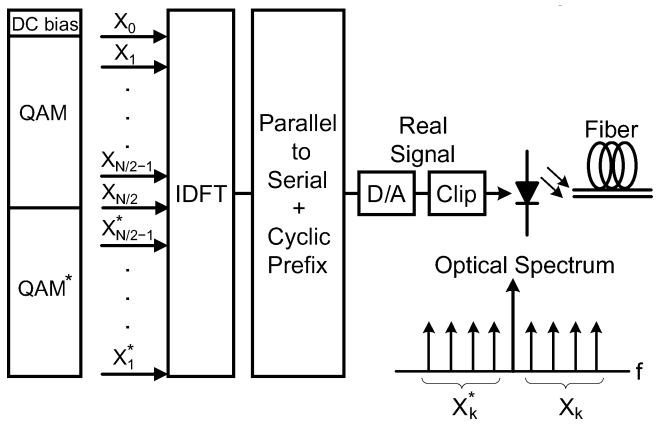

Fig. 4. Block diagram of a DC-OFDM transmitter.

We note that when the total average transmitted power is constrained, the optimal power allocation yields a variable data rate. For some applications, a fixed data rate is required. In this case, the optimal design minimizes the average power required to transmit at a given fixed bit rate. The power minimization can be written as

$$\min_{\mathrm{P_n}} \mathrm{P_t} = \sum_{n=0}^{N-1} P_n$$
$$\text{subject to } \mathrm{b} = \sum_{n=0}^{N-1} \log_2\left(1 + \frac{P_n |H_n|^2}{\Gamma \sigma_n^2}\right). \tag{7}$$

The solution of (7) is also the water-filling solution given by (5). However, in this case the constant a is chosen such that bit rate is equal to the desired value. We can interpret this solution as the water/power being poured until the required bit rate is achieved.

III. OFDM System Model

The OFDM system model is shown in Fig. 3.

An optical OFDM modulator encodes transmitted symbols onto an electrical OFDM waveform and modulates this onto the intensity (instantaneous power) of an optical carrier. The modulator can generate one of DC-OFDM, SSB-OFDM or ACO-OFDM. Details of modulators for particular OFDM schemes are described in Section IV. After propagating through the SMF, the optical signal is optically amplified and bandpass-filtered. We assume that the optical amplifier has a high gain so that its amplified spontaneous emission (ASE) is dominant over thermal and shot noises. The ASE noise is modeled as complex additive white Gaussian noise (AWGN) with zero mean. The ASE can be expressed as $n_{\mathrm{ASE}}(t) = n_I(t) + j \cdot n_Q(t)$, where $n_I(t)$ and $n_Q(t)$ are uncorrelated Gaussian random processes, each having half the variance of $n_{\mathrm{ASE}}(t)$.

In our analysis, PMD and fiber nonlinearity are neglected, and GVD is the only fiber impairment considered. In the optical electric field domain, the fiber is modeled as a linear system with transfer function given by

$$H_{\mathrm{fiber}}(\omega) = e^{j\omega^2 \frac{\beta_2}{2} L}, \tag{8}$$

where β_2 is the fiber GVD parameter and L is the fiber length. The overall optical transfer function is given by

$$H(\omega) = H_{\mathrm{fiber}}(\omega) \cdot H_{\mathrm{filter}}(\omega), \tag{9}$$

where $H_{\mathrm{filter}}(\omega)$ is the transfer function of the optical bandpass filter.

After bandpass filtering, the optical signal intensity is detected, and the electrical current is lowpass filtered. The OFDM signal is demodulated and equalized with a single-tap equalizer on each subcarrier to compensate for the channel distortion [6], [7].

IV. Analysis of Direct-Detection OFDM Schemes

A. DC-Clipped OFDM

The main disadvantage of using OFDM with IM is the required DC bias to make the OFDM signal nonnegative. Since OFDM signals have a high peak-to-average power ratio, the required DC bias can be excessively high. A simple approach to reduce the DC offset is to perform hard-clipping on the negative signal peaks [5], [6]. This technique is usually called DC-OFDM and the transmitter is shown in Fig. 4.

In Fig. 4, the transmitted symbols are modulated such that the time-domain waveform is real. This is achieved by enforcing Hermitian symmetry in the symbols input to the inverse discrete Fourier transform (IDFT). We note that the 0th or the DC subcarrier is not modulated and it is equal to the DC offset. After D/A conversion, the electrical OFDM signal is hard-clipped such that the waveform is nonnegative and then the signal is intensity modulated onto the optical carrier.

After propagating through the optical system, the detected signal can be written as

$$y_{\mathrm{det}}(t) = |E(t)|^2 = |\sqrt{x(t)} \otimes h(t)|^2, \tag{10}$$

where $E(t)$ is the output electric field, $x(t)$ is the DC-OFDM signal and $h(t)$ is the impulse response of the overall optical system, given by the inverse Fourier transform of (9). For now, we have neglected amplifier noise in (10).

We can expand the OFDM signal as $x(t) = A + x_{\mathrm{ac}}(t) + n_{\mathrm{clip}}(t)$, where A is the average of the OFDM signal after clipping and $x_{\mathrm{ac}}(t)$ is the OFDM signal with the DC subcarrier equal to zero and $n_{\mathrm{clip}}(t)$ is the clipping noise. We note that if the DC bias is chosen such that there is no clipping, then A is

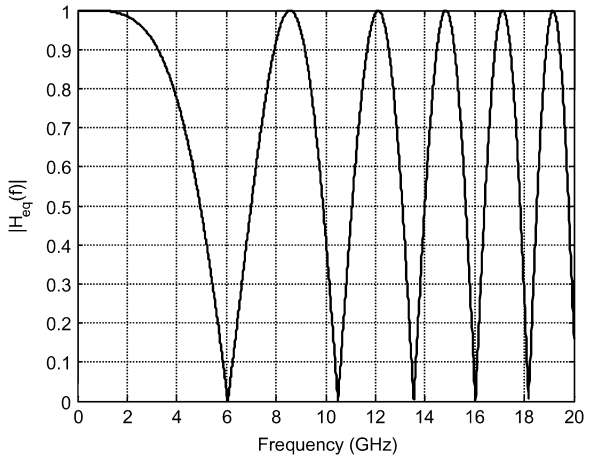

Fig. 5. Equivalent transfer function for DC-OFDM for $R = 20$ Gbit/s, $L = 100$ km and $D = 17$ ps/nm/km, corresponding to $\gamma = 0.87$.

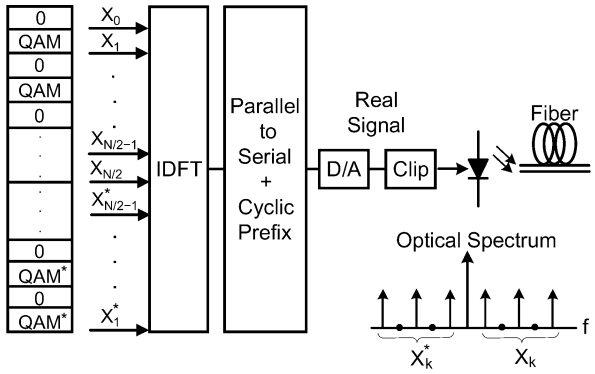

Fig. 6. Block diagram of an ACO-OFDM transmitter.

equal to the DC bias and $n_{\text{clip}}(t) = 0$. For now, we neglect the clipping noise. The detected signal is then

$$y_{\text{det}}(t) = |\sqrt{A + x_{\text{ac}}(t)} \otimes h(t)|^2. \tag{11}$$

We can now use the Taylor series expansion on the square-root term. The detected signal becomes

$$y_{\text{det}}(t) = \left[\left(\sqrt{A} + \frac{x_{\text{ac}}(t)}{2\sqrt{A}} - \frac{x_{\text{ac}}^2(t)}{8A^{3/2}} + \cdots\right) \otimes h(t)\right] \times \left[\left(\sqrt{A} + \frac{x_{\text{ac}}(t)}{2\sqrt{A}} - \frac{x_{\text{ac}}^2(t)}{8A^{3/2}} + \cdots\right) \otimes h(t)\right]^* \tag{12}$$

After expanding the terms in (12), the detected signal simplifies to

$$y_{\text{det}}(t) = A + \frac{x_{\text{ac}}(t) \otimes h(t)}{2} + \frac{x_{\text{ac}}^*(t) \otimes h^*(t)}{2} - \frac{x_{\text{ac}}^2(t) \otimes h(t)}{8A} - \frac{x_{\text{ac}}^{2*}(t) \otimes h^*(t)}{8A} + \cdots \tag{13}$$

The first two convolution terms in (13) correspond to an equivalent linear channel. The remaining terms in (13) correspond to the interaction between the detector nonlinearity and the fiber GVD. They can be interpreted as an equivalent nonlinear detection noise that will degrade the receiver SNR. We note that these terms decrease as the bias level increases.

The linear terms in (13) can be further simplified since the OFDM signal is real valued, i.e., $x_{\text{ac}}(t) = x_{\text{ac}}^*(t)$. Thus, we can write the equivalent linear channel for DC-OFDM as

$$h_{\text{eq}}(t) = \frac{h(t) + h^*(t)}{2}. \tag{14}$$

The transfer function is then

$$H_{\text{eq}}(\omega) = \frac{e^{j\omega^2 \frac{\beta_2}{2} L} + e^{-j\omega^2 \frac{\beta_2}{2} L}}{2} = \cos\left(\omega^2 \frac{\beta_2}{2} L\right). \tag{15}$$

The equivalent transfer function is plotted on Fig. 5.

In Fig. 5, we observe that the equivalent channel transfer function is not unitary and is frequency-selective. Thus, in order to maximize the bit rate, we need to use variable bit loading on each subcarrier.

B. Asymmetrically Clipped Optical OFDM

Armstrong and Lowery [5], [6] proposed adding no DC bias and clipping the entire negative excursion of an electrical OFDM signal before modulating it onto the intensity of an optical carrier. They showed that clipping noise is avoided (at least in the absence of dispersion) by encoding information symbols on only the odd subcarriers. This technique is called ACO-OFDM. Fig. 6 shows a block diagram of an ACO-OFDM transmitter.

As in DC-OFDM, the OFDM subcarriers are assumed to have Hermitian symmetry, so that the time-domain waveform is real. Because only the odd subcarriers are used to transmit data, for a given choice of signal constellation, ACO-OFDM has only half the spectral efficiency of DC-OFDM. After D/A conversion, the electrical OFDM signal is hard-clipped at zero and intensity modulated onto an optical carrier.

The equivalent transfer function of ACO-OFDM is the same as DC-OFDM, and is given by (15). This can be shown by using the same approach as in the previous section, setting A equal to the average of the ACO-OFDM waveform.

C. Single-Sideband OFDM

Another approach to reducing the required DC bias is to use SSB-OFDM. In SSB-OFDM, only one of the DC-OFDM sidebands is transmitted and there is a frequency guard band between the sideband and the optical carrier. The bandwidth of the guard band must be no smaller than that of the OFDM sideband. Fig. 7 shows a block diagram of a digital implementation of a SSB-OFDM transmitter.

SSB-OFDM can be obtained by applying a Hilbert transform to a DC-OFDM signal. A Hilbert transform can be generated at the OFDM transmitter by setting the negative subcarriers to zero, as shown in Fig. 7. The frequency guard band is obtained by modulating the high-frequency subcarriers and setting to zero the low-frequency subcarriers. The IDFT output is an analytical signal, and its real and imaginary components are used for the drive voltages of the inphase and quadrature inputs of a quadrature Mach–Zehnder modulator. Hence, contrary to the previous techniques, in SSB-OFDM the signal is actually modulated onto the optical electric field, and not simply onto its intensity, and therefore no hard clipping is required. The DC

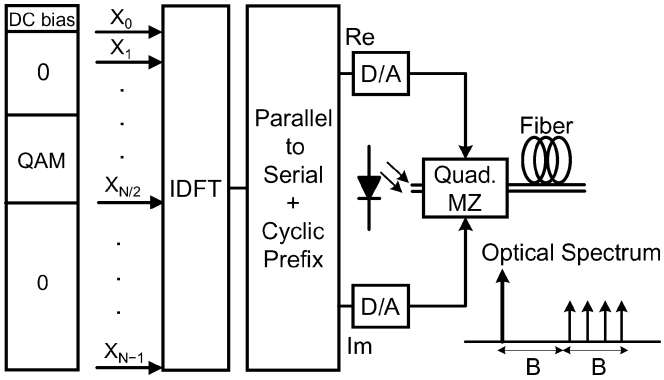

Fig. 7. Block diagram of an SSB-OFDM transmitter.

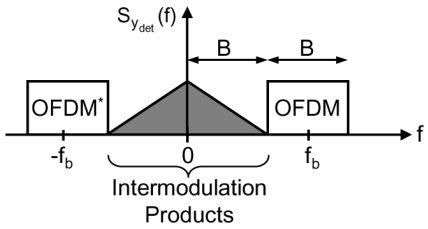

Fig. 8. PSD of the detected signal in SSB-OFDM.

bias in SSB-OFDM sets the amplitude of the optical carrier, affecting system performance, as we show in the following.

SSB-OFDM has the same optical spectral efficiency as DC-OFDM. However, the transmitter considered here requires twice the bandwidth of DC-OFDM for a digital implementation of SSB-OFDM. Other transmitter implementations that require less bandwidth are discussed in [8]. There have been some studies on the optimization of SSB-OFDM, particularly in the trade-off between spectral efficiency and performance as a function of the optical carrier power (i.e., DC bias) [12], [13]. However, in the previous work, the DC bias and the powers of the subcarriers were not jointly optimized based on the channel response and the nonlinear beat noises.

After propagating through the optical system, the detected signal can be written as

$$y_{\rm det}(t) = |E(t)|^2 = |(A + s(t)e^{j2\pi f_b t}) \otimes h(t)|^2, \qquad (16)$$

where $s(t)e^{j2\pi f_b t}$ is the OFDM sideband centered at frequency f_b, A is the DC bias and $h(t)$ is the optical channel impulse response, given by the inverse Fourier transform of (9). We can expand the detected signal as

$$\begin{aligned} y_{\rm det}(t) &= [(A + s(t)e^{j2\pi f_b t}) \otimes h(t)] \\ &\quad \cdot [(A + s(t)e^{j2\pi f_b t}) \otimes h(t)]^* \\ &= |A|^2 + A \cdot s(t)e^{j2\pi f_b t} \otimes h(t) \\ &\quad + A \cdot s^*(t)e^{-j2\pi f_b t} \otimes h^*(t) \\ &\quad + |s(t) \otimes h(t)|^2 \end{aligned} \qquad (17)$$

Assuming that the OFDM sideband has a bandwidth B centered at f_b, the quadratic term in (17) occupies a bandwidth from $-B$ to $+B$. Thus, if the frequency guard band is equal or greater than B, the quadratic intermodulation products are avoided. This concept is illustrated in Fig. 8.

Finally, since the quadratic intermodulation products are avoided by using the guard band and the desired signal is the OFDM sideband centered at frequency f_b, we conclude from (17) that the transfer function for SSB-OFDM is a scaled version of the optical transfer function given by (9), and can be written as

$$H_{\rm SSB}(\omega) = A \cdot H(\omega), \qquad (18)$$

where A is the DC bias.

D. Effects of Amplifier Noise

If we include amplifier noise, the detected signal can be written as

$$y_{\rm det}(t) = |E(t) + n(t)|^2, \qquad (19)$$

where $E(t)$ is the output electric field and $n(t)$ is the filtered ASE, i.e., $n(t) = n_{\rm ASE}(t) \otimes h_{\rm filter}(t)$.

We can further expand the detected signal as

$$\begin{aligned} y_{\rm det}(t) &= (E(t) + n(t)) \cdot (E(t) + n(t))^* \\ &= |E(t)|^2 + E(t) \cdot n^*(t) + E^*(t) \cdot n(t) + |n(t)|^2. \end{aligned} \qquad (20)$$

From (20), we observe that the signal is corrupted by signal-spontaneous and spontaneous-spontaneous beat noises. We define $w(t) = E(t) \cdot n^*(t) + E^*(t) \cdot n(t) + |n(t)|^2$ as the total noise. By using the moment generating function for $n(t)$ or Gaussian moments theorems [14] and assuming that the transmitted signal is uncorrelated with the amplifier noise, we can write the autocorrelation of the total noise $w(t)$ as

$$\begin{aligned} R_{ww}(\tau) &= \left(R_{E'E'}(\tau) + |m_E|^2\right) \cdot R^*_{nn}(\tau) \\ &\quad + \left(R^*_{E'E'}(\tau) + |m_E|^2\right) \cdot R_{nn}(\tau) \\ &\quad + R^2_{n_I n_I}(0) + 2R^2_{n_I n_I}(\tau), \end{aligned} \qquad (21)$$

where $E'(t) = E(t) - m_E, m_E$ is the average value of the received electric field, $R_{E'E'}(\tau)$ is the autocorrelation of $E'(t), R_{nn}(\tau)$ is the autocorrelation of the noise $n(t)$ and $R_{n_I n_I}(\tau)$ is the autocorrelation of the real component of $n(t)$.

In (21), there are three main noise components:

- DC-spontaneous noise: $|m_E|^2 \cdot (R^*_{nn}(\tau) \cdot + R_{nn}(\tau))$
- Signal-spontaneous noise: $R_{E'E'}(\tau) \cdot R^*_{nn}(\tau) + R^*_{E'E'}(\tau) \cdot R_{nn}(\tau)$
- Spontaneous-spontaneous noise: $R^2_{n_I n_I}(0) + 2R^2_{n_I n_I}(\tau)$

From (21), we observe that the DC-spontaneous beat noise power increases proportionally with the DC bias. In DC-OFDM, if the DC bias is excessively high, the DC-spontaneous beat noise dominates, and the receiver SNR is low. On the other hand, if the DC bias is small, the clipping noise and the nonlinear detection noise from (13) dominate, and the receiver SNR is also low. Thus, the DC bias needs to be optimized for best performance.

In SSB-OFDM, if the DC bias is high, the receiver SNR is unaffected since both the OFDM signal and the dominant noise are amplified by the DC offset. However, the optical power efficiency is very low in this case. On the other hand, if the DC bias

TABLE I
ELECTRICAL AND OPTICAL BANDWIDTHS REQUIRED TO TRANSMIT AT A BIT RATE R

Modulation	Receiver BW	Optical BW
OOK	R	$2R$
DC-OFDM	R	$2R$
ACO-OFDM	R	$2R$
SSB-OFDM	$2R$	$2R$

is small, the other noise terms dominate and the receiver SNR is low.

V. COMPARISON OF DIRECT-DETECTION MODULATION FORMATS

In order to make our results independent of bit rate, we use the dimensionless dispersion index γ, defined as

$$\gamma = |\beta_2| R^2 L, \tag{22}$$

where β_2 is the fiber GVD parameter, L is the fiber length and R is the bit rate. Furthermore, in order for the required optical SNR to be independent of the bit rate, the noise bandwidth should be matched to the signal bandwidth. Thus, we use the normalized optical SNR defined as

$$\mathrm{SNR}_{\mathrm{opt}} = \frac{P_{\mathrm{opt}}}{N_0 R}, \tag{23}$$

where P_{opt} is the optical power, N_0 is the ASE power spectral density and R is the bit rate. The normalized optical SNR is related to the conventional optical SNR (OSNR) measured in a 0.1-nm (12.5-GHz) bandwidth as

$$\mathrm{SNR}_{\mathrm{opt}} = \mathrm{OSNR} \frac{12.5\ \mathrm{GHz}}{R}. \tag{24}$$

The system model is shown in Fig. 3. As mentioned before, we neglect all transmission impairments except for GVD. We consider a fiber with a dispersion $D = 17$ ps/(nm·km). The optical filter is modeled as a second-order super-Gaussian filter with a 3-dB bandwidth $B_0 = 35$ GHz, which is realistic for commercial systems with 50-GHz channel spacing. We also assume that the optical amplifier has a high gain so that the ASE is dominant over thermal and shot noises from the receiver. At the receiver, the antialiasing filter is a fifth-order Butterworth lowpass filter having a 3-dB cutoff frequency equal to the first null of the OFDM spectrum [15].

In order to perform a fair comparison with OOK, we maintain OFDM optical bandwidth constant and equal to the optical bandwidth required to transmit at a bit rate R using OOK. Table I summarizes the required electrical and optical bandwidths for the different modulation techniques.

For all the OFDM formats, we use an oversampling ratio of $M_s = 64/52 \approx 1.2$ to avoid aliasing. As an initial estimate, we choose the cyclic prefix and the number of subcarriers using the equivalent linear channel described in Section IV for each OFDM format [15]. Then, we increase the cyclic prefix until the interference penalty is completely eliminated. Typically, the final result is very close to the initial estimate.

After selecting the OFDM parameters, we proceed to optimally allocate power among the subcarriers. We note that we cannot use (5) and (6) directly, since the nonlinear detection noise in each subcarrier depends on the power of all the subcarriers. Thus, we perform the power allocation iteratively. For a given power allocation, the SNR measured at each subcarrier is used to compute an updated water-filling solution. We repeat this process until the power allocation no longer changes. In our simulations, we do not actually implement the coding required to transmit the number of bits given by the water-filling solution. In practice, the constellation used on each subcarrier will be M-ary QAM (M-QAM) with coding (e.g., trellis coded modulation) in order to achieve the number of bits given by the water-filling algorithm. As seen before, the number of bits that can be allocated to a subcarrier depends only on the received SNR of that subcarrier. For simplicity, we used QPSK on each subcarrier with the same power given by the water-filling solution in order to obtain the same SNR that would be required to transmit the specific number of bits given by the bit allocation.

In addition to optimizing the power/bit allocation at each subcarrier, we need to optimize the DC bias for DC-OFDM and SSB-OFDM. In order to minimize the DC bias, we use a bias level proportional to the square-root of the electrical power. We define the proportionality constant as the bias ratio (BR), which is given by

$$\mathrm{BR} = \frac{\mathrm{DC}_{\mathrm{bias}}}{\sigma}, \tag{25}$$

where $\sigma = \sqrt{P_{\mathrm{elect}}}$ is the standard deviation of the electrical OFDM waveform. Using the BR insures that the water-filling solution minimizes the DC bias, and thus the optical power required. For example, in DC-OFDM, if the electrical power is excessively high, the DC bias will also be excessively high. A high DC bias reduces both the clipping noise and the intermodulation terms, and therefore the received SNR on each subcarrier is high. On the next iteration, the water-filling algorithm removes some of the excess electric power in order to lower the SNR to the desired value, and therefore the DC bias decreases. On the other hand, if the DC bias is too low, the clipping noise and the intermodulation terms are excessively high, and therefore the received SNR on each subcarrier is too low. On the next iteration, the water-filling algorithm adds more electric power in order to increase the SNR to the desired value, and consequently the DC bias increases. The same reasoning can be applied for SSB-OFDM. The minimum required optical SNR is obtained by performing an exhaustive search on the BR value, as shown on Fig. 9.

Finally, we note that the water-filling solution is optimum for Gaussian noise but the noises in an optically amplified direct-detection receiver are not Gaussian. However, if the number of subcarriers is large, we expect the noise to be approximately Gaussian after the DFT, an assumption confirmed in our simulations.

Typical high-performance FEC codes for optical systems have a threshold of the order of $P_b = 10^{-3}$, so we compute the minimum optical power required to achieve $P_b = 10^{-3}$ for the different OFDM formats. Fig. 9 shows the normalized

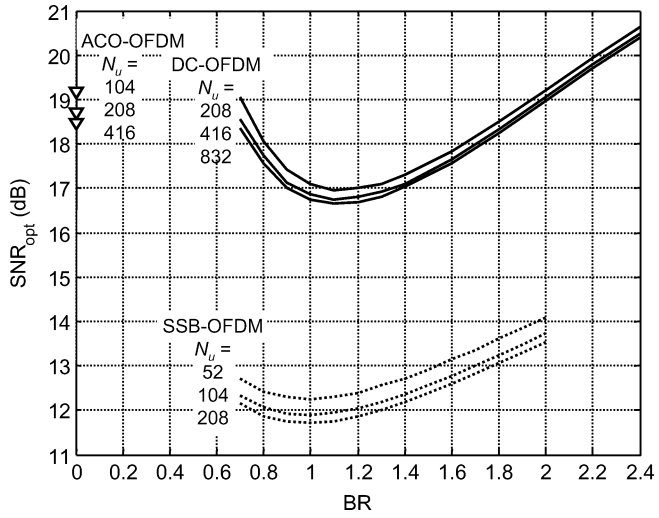

Fig. 9. Normalized optical SNRs required for the different OFDM formats for $\gamma = 0.25$ to achieve $P_b = 10^{-3}$. The number of used subcarriers, N_u, is indicated for each curve.

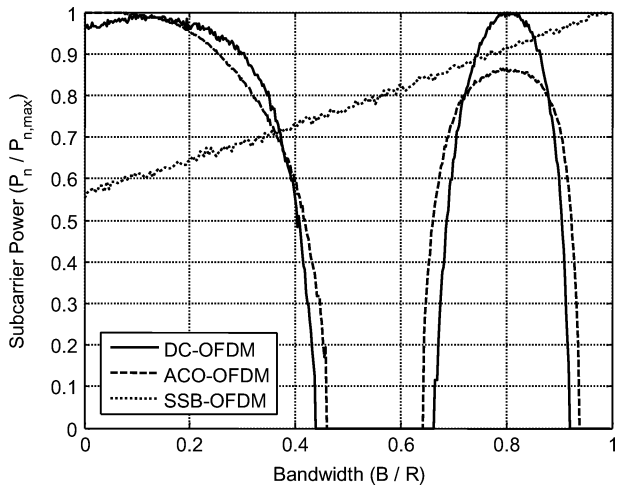

Fig. 10. Subcarrier power distribution for DC-OFDM, ACO-OFDM, SSB-OFDM and to achieve a $P_b = 10^{-3}$ for $\gamma = 0.25$. The number of used subcarriers is 416, 416 and 208 for DC-OFDM ($\mathrm{BR} = 1.1$), ACO-OFDM and SSB-OFDM ($\mathrm{BR} = 1.0$), respectively.

optical SNR required for a dispersion index of $\gamma = 0.25$. As an example, $\gamma = 0.25$ corresponds to 100 km of standard single-mode fiber (SSMF) without optical dispersion compensation at 10 Gbit/s or 70 km of SSMF with 90% inline dispersion compensation at 40 Gbit/s.

In Fig. 9, we notice that for all OFDM formats the required optical SNR decreases slightly with the number of subcarriers, since the prefix penalty decreases as the number of subcarriers increases. In addition, OFDM uses the available channel bandwidth more efficiently as the number of subcarriers increases, which contributes to the reduction of the required optical SNR. In Fig. 9, we observe that the performance achieved with the chosen number of subcarriers is very close to the best performance achievable for each OFDM technique.

We also verify that SSB-OFDM requires the lowest optical SNR to achieve $P_b = 10^{-3}$. Furthermore, for SSB-OFDM, the required optical SNR increases linearly with the DC bias for BR values greater than 1.4. This is expected since from (18) the electrical SSB OFDM signal is scaled by the DC bias, and the dominant noise for a high bias level is the DC-spontaneous beat noise. As we decrease the BR, the signal-spontaneous beat noise is no longer negligible, and the minimum required optical SNR is achieved at a $\mathrm{BR} = 1$. We note that the optimum BR is independent of the number of used subcarriers. If we further decrease the BR, more power has to be allocated to each subcarrier to compensate for the signal-spontaneous beat and therefore the required optical SNR increases.

For DC-OFDM, the required optical SNR also increases linearly with the DC bias for BR values greater than 1.6, since the dominant noise is the DC-spontaneous beat noise. As we decrease the BR, the clipping and the nonlinear detection noises are no longer negligible and the minimum required optical SNR is achieved at a $\mathrm{BR} = 1.1$. We note again that the optimum BR is independent of the number of used subcarriers. If we further decrease the BR, more power must be allocated to each subcarrier to compensate for the clipping and nonlinear noise, and therefore the average value of the OFDM waveform increases. Thus, the required optical SNR also increases.

Fig. 10 shows an example of the subcarrier power allocation for the different OFDM formats.

We observe that the power allocation is consistent with the equivalent linear channel described in Section IV. For DC-OFDM and ACO-OFDM, we observe a frequency-selective channel with notches, as expected. For SSB-OFDM, there are no notches, and the power allocation follows the shape of the signal-spontaneous beat noise.

For DC-OFDM, we can obtain an analytical lower bound on the required optical SNR by assuming that the dominant noises are the DC-spontaneous and the spontaneous-spontaneous beat noises from (21) and by using the equivalent linear channel from (15). If we fix the DC bias, the optimum power allocation is given directly by (5) and (6), since the noises do not depend on the subcarrier powers. Fig. 11 compares the analytical lower bound with the results obtained by simulation.

From Fig. 11, we verify that for high BR ($\mathrm{BR} > 2$), the lower bound is equal to the simulation results. Thus, we conclude that using water-filling iteratively with the BR normalization for the DC level converges to the optimum power allocation in the linear regime. Furthermore, from Figs. 9 and 11, we observe that DC-OFDM can never be more power efficient than SSB-OFDM.

Fig. 12 shows the minimum required optical SNR for various dispersion indexes γ. The OFDM parameters are summarized in Table IV.

In Fig. 12, we observe that SSB-OFDM requires the lowest optical SNR to achieve $P_b = 10^{-3}$. The high performance of SSB-OFDM comes at the price of the extra electrical bandwidth required to avoid the quadratic intermodulation products. Furthermore, unlike OOK with MLSD, SSB-OFDM requires two D/As and a quadrature modulator at the transmitter.

From Fig. 12, we can also verify that the required optical SNR for ACO-OFDM is higher than DC-OFDM for γ greater than

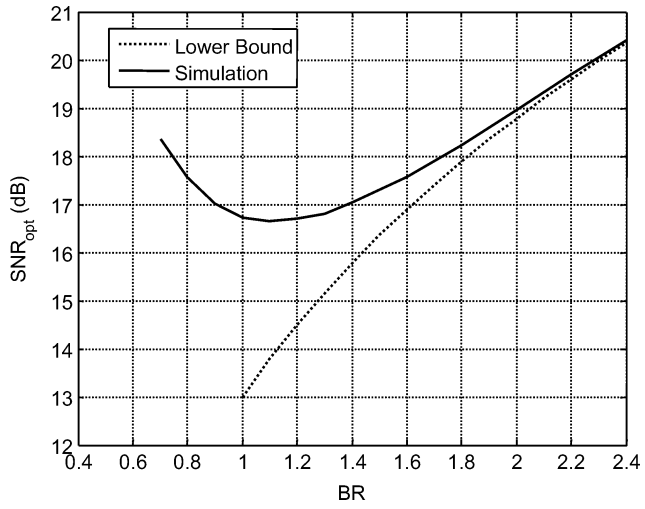

Fig. 11. Normalized optical SNR required for DC-OFDM to achieve $P_b = 10^{-3}$ for $\gamma = 0.25$. The number of used subcarriers is $N_u = 832$.

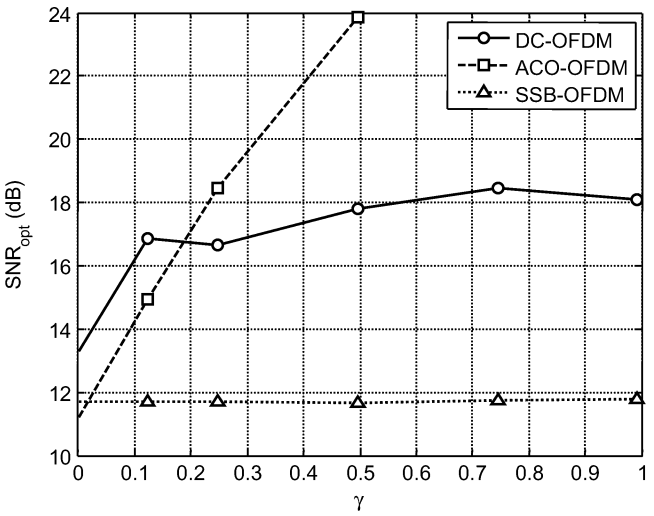

Fig. 12. Minimum normalized optical SNR required for various dispersion indexes γ for the different OFDM formats.

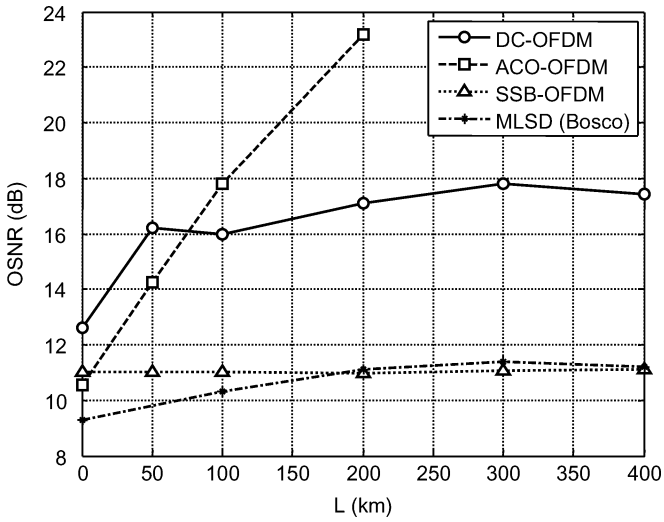

Fig. 13. OSNR values (over 0.1 nm) required to obtain $P_b = 10^{-3}$ at 10.7 Gbit/s for OFDM and for OOK with MLSD [4].

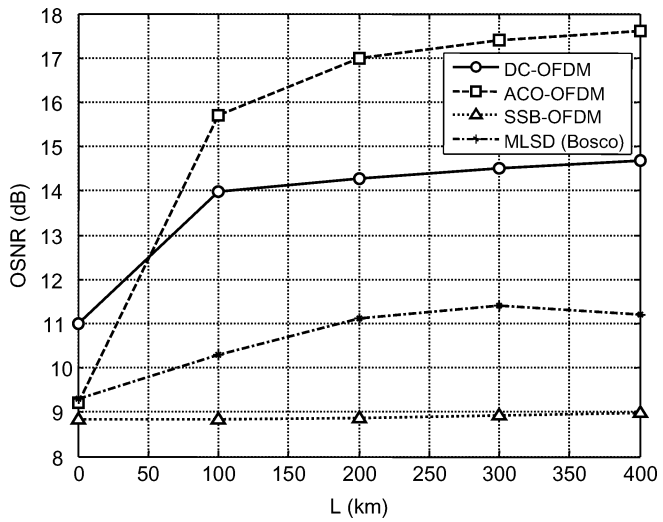

Fig. 14. OSNR values (over 0.1 nm) required to obtain $P_b = 10^{-3}$ at 10.7 Gbit/s for OFDM and for OOK with MLSD [4]. In this case, the OFDM signal occupies the full channel bandwidth ($B_0 = 35$ GHz).

0.25. This happens because the fiber dispersion destroys the orthogonality between the subcarriers and therefore there is significant nonlinear inter-carrier interference (ICI). Furthermore, since half the subcarriers are zero, the used subcarriers need to transmit at twice the data rate, which exacerbates the ICI. We note that the power allocation for ACO-OFDM does not converge for γ greater than 0.5. On the other hand, for low dispersion the subcarriers remain orthogonal and the ICI is avoided due to the zero subcarriers. In this regime, ACO-OFDM performs better than DC-OFDM.

In order to compare OFDM with single-carrier, we use results on OOK with MLSD from [4], since OOK with MLSD achieves the best optical power efficiency among known IM/DD techniques. For ease of comparison with [4], we present our results for 10.7 Gbit/s in Fig. 13 using the conventional definition of optical SNR measured over a 12.5-GHz band (OSNR) to achieve $P_b = 10^{-3}$.

We see that OOK with MLSD performs better than DC-OFDM or ACO-OFDM. SSB-OFDM performs as well as OOK with MLSD but requires twice the electrical bandwidth. For 10 Gbit/s systems, we can further optimize the OFDM signals by using the full available optical bandwidth ($B_0 = 35$ GHz). In this case, we are trading optical bandwidth for optical power. Fig. 14 shows the OSNR required to obtain $P_b = 10^{-3}$ when the OFDM signal occupies the full channel bandwidth ($B_0 = 35$ GHz).

As we can observe, SSB-OFDM performs better than MLSD if we use the extra available optical bandwidth. We also notice that the power allocation for ACO-OFDM converges because of the extra degrees of freedom as compared to the case in Fig. 13. However, OOK with MLSD still performs better than ACO-OFDM and DC-OFDM.

Another important criterion is the computational complexity of a modulation/detection technique. For OOK with MLSD, the complexity of the Viterbi algorithm depends on the number of trellis states, given by $N = 2^M$, where M is the channel

TABLE II
MEMORY REQUIRED FOR VARIOUS VALUES OF THE DISPERSION INDEX γ FOR OOK WITH MLSD [4]

γ	0.25	0.5	0.75	1
M	3	5	6	8

TABLE III
NUMBER OF REAL OPERATIONS REQUIRED PER BIT FOR SSB-OFDM AND OOK WITH MLSD FOR THE VARIOUS DISPERSION INDEXES γ

γ	MLSD	SSB-OFDM		
	Receiver	Transmitter	Receiver	Total
0.25	32	47.9	48.8	96.7
0.5	128	46.8	47.8	94.6
0.75	256	52.1	53.1	105.2
1	1024	51.5	52.4	103.9

memory measured in bit intervals. In the Viterbi algorithm, complexity is dominated by computation of the branch metrics. In each bit interval, $2 \cdot N \cdot K$ branch metrics must be evaluated by the receiver, where K is the number of samples per bit interval [4]. Thus, the complexity per second for OOK with MLSD is at least $2 \cdot N \cdot K/T_b$, where T_b is the bit interval. The complexity order per bit for OOK with MLSD is then at least

$$O_{\mathrm{MLSD},T_b}(M) = 2 \cdot 2^M \cdot K. \tag{26}$$

In our case, $K = 2$ and the memory M required for different values of dispersion index γ are listed in Table II [4].

For OFDM, the IDFT and DFT operations are performed efficiently using a fast Fourier transform (FFT) algorithm. A FFT requires $4 \cdot N \cdot \log_2(N)$ real operations (multiplications plus additions), where N is the FFT size. Specifically, the number of additions is $8/3 \cdot N \cdot \log_2(N)$ and the number of multiplications is $4/3 \cdot N \cdot \log_2(N)$ [16]. Thus, the number of real operations required per second for the transmitter is $4 \cdot N \cdot \log_2(N)/T_{\mathrm{OFDM}}$, where T_{OFDM} is the OFDM symbol period, which is given in [15]. For the OFDM receiver, we need to take into account the complex single-tap equalizer on each used subcarrier. Hence, the number of real operations required per second for the receiver is $4(N \cdot \log_2(N) + N_u)/T_{\mathrm{OFDM}}$, where $N_u$is the number of used subcarriers. The overall complexity order per bit for OFDM is

$$\begin{aligned} O^{\mathrm{Tx}}_{\mathrm{OFDM},T_b}(N) &= \log_2(N) T_b/T_{\mathrm{OFDM}} \\ O^{\mathrm{Rx}}_{\mathrm{OFDM},T_b}(N) &= [N \log_2(N) + N_u] T_b/T_{\mathrm{OFDM}} \end{aligned} \tag{27}$$

where $R = 1/T_b$ is the bit rate.

Using data from Tables IV and II and (26) and (27), in Table III we compare the computational complexity per bit for SSB-OFDM and OOK with MLSD.

We observe that SSB-OFDM requires fewer operations per bit than OOK with MLSD. The relatively low complexity of OFDM is due to the efficiency of the FFT algorithm. The high complexity of OOK with MLSD is caused by the exponential dependence of the number of trellis states on the channel memory length.

TABLE IV
OFDM PARAMETERS FOR THE VARIOUS DISPERSION INDEXES γ. N IS THE DFT SIZE, N_u IS THE NUMBER OF USED SUBCARRIERS AND ν IS THE CYCLIC PREFIX

γ	DC-OFDM	ACO-OFDM	SSB-OFDM
0.25	$N = 2048$ $N_u = 832$ $\nu = 18$	$N = 2048$ $N_u = 416$ $\nu = 18$	$N = 1024$ $N_u = 208$ $\nu = 11$
0.5	$N = 2048$ $N_u = 832$ $\nu = 31$	$N = 2048$ $N_u = 416$ $\nu = 31$	$N = 1024$ $N_u = 208$ $\nu = 21$
0.75	$N = 2048$ $N_u = 832$ $\nu = 44$	$N = 2048$ $N_u = 416$ $\nu = 44$	$N = 2048$ $N_u = 416$ $\nu = 32$
1	$N = 2048$ $N_u = 832$ $\nu = 59$	$N = 2048$ $N_u = 416$ $\nu = 59$	$N = 2048$ $N_u = 416$ $\nu = 42$

VI. CONCLUSION

We have evaluated the performance of three different OFDM formats in amplified DD optical systems: SSB-OFDM, DC-OFDM and ACO-OFDM. We have derived equivalent linear channel models for each format in the presence of GVD. We showed how to minimize the average optical power required to achieve a specified error probability by iteratively adjusting the subcarrier power allocation and the bias ratio. We found that for a given dispersion, SSB-OFDM requires the smallest optical power. We presented an analytical lower bound for the minimum required optical SNR for DC-OFDM and concluded that DC-OFDM can never achieve the same optical power efficiency as SSB-OFDM. We showed that at low dispersion, ACO-OFDM performs close to SSB-OFDM but at high dispersion ACO-OFDM performs worse than DC-OFDM, because of nonlinear ICI. Using published results on OOK with MLSD, we showed that SSB-OFDM can achieve the same optical power efficiency as OOK with MLSD, at the expense of requiring twice the electrical bandwidth and therefore requiring also an higher A/D sampling rate. Furthermore, SSB-OFDM requires a quadrature modulator, which also increases the hardware complexity. On the other hand, we showed that SSB-OFDM requires significantly lower computational complexity than OOK with MLSD.

ACKNOWLEDGMENT

The authors would like to thank A. P. T. Lau and E. Ip for helpful discussions and suggestions.

REFERENCES

[1] E. Ip and J. M. Kahn, "Digital equalization of chromatic dispersion and polarization mode dispersion," *J. Lightw. Technol.*, vol. 25, no. 8, pp. 2033–2043, Aug. 2007.

[2] O. E. Agazzi, M. R. Hueda, H. S. Carrer, and D. E. Crivelli, "Maximum-likelihood sequence estimation in dispersive optical channels," *J. Lightw. Technol.*, vol. 23, no. 2, pp. 749–763, Feb. 2005.

[3] T. Foggi, E. Forestieri, G. Colavolpe, and G. Prati, "Maximum-likelihood sequence detection with closed-form metrics in OOK optical systems impaired by GVD and PMD," *J. Lightw. Technol.*, vol. 24, no. 8, pp. 3073–3087, Aug. 2006.

[4] G. Bosco, P. Poggiolini, and M. Visintin, "Performance analysis of MLSE receivers based on the square-root metric," *J. Lightw. Technol.*, vol. 26, no. 14, pp. 2098–2109, Jul. 2008.
[5] J. Armstrong, B. J. C. Schmidt, D. Kalra, H. A. Suraweera, and A. J. Lowery, "Performance of asymmetrically clipped optical OFDM in AWGN for an intensity modulated direct detection system," *Proc. IEEE GLOBECOM*, 2006.
[6] J. Armstrong and B. J. C. Schmidt, "Comparison of asymmetrically clipped optical OFDM and DC-biased optical OFDM in AWGN," *IEEE Commun. Lett.*, vol. 12, no. 5, pp. 343–345, 2008.
[7] A. J. Lowery, "Improving sensitivity and spectral efficiency in direct-detection optical OFDM systems," in *Proc. OFC/NFOEC 2008*, 2008, Paper OMM4.
[8] B. J. C. Schmidt, A. J. Lowery, and J. Armstrong, "Experimental demonstrations of electronic dispersion compensation for long-haul transmission using direct-detection optical OFDM," *J. Lightw. Technol.*, vol. 26, no. 1, pp. 196–203, Jan. 2008.
[9] J. M. Cioffi, G. P. Dudevoir, M. V. Eyuboglu, and G. D. Forney, Jr. , "MMSE decision-feedback equalizers and coding—Part II: Coding results," *IEEE Trans. Commun.*, vol. 43, no. 10, pp. 2595–2604, Oct. 1995.
[10] G. D. Forney and G. Ungerboeck, "Modulation and coding for linear Gaussian channels," *IEEE Trans. Inf. Theory*, vol. 44, no. 6, pp. 2384–2415, Jun. 1998.
[11] W. Yu, G. Ginis, and J. M. Cioffi, "An adaptive multiuser power control algorithm for VDSL," *Proc. IEEE GLOBECOM*, 2001.
[12] A. Ali, J. Leibrich, and W. Rosenkranz, "Spectral efficiency and receiver sensitivity in direct detection optical-OFDM," *Proc. OFC/NFOEC 2009*, 2009, Paper OMT7.
[13] A. Ali, H. Paul, J. Leibrich, W. Rosenkranz, and K. D. Kammeyer, "Optical biasing in direct detection optical-OFDM for improving receiver sensitivity," in *Proc. OFC/NFOEC 2010*, 2010, Paper JThA12.
[14] J. W. Goodman, *Statistical Optics*. Hoboken, NJ: Wiley-Interscience, 1985.
[15] D. J. F. Barros and J. M. Kahn, "Optimized dispersion compensation using orthogonal frequency-division multiplexing," *J. Lightw. Technol.*, vol. 26, no. 16, pp. 2889–2898, Aug. 2008.
[16] S. G. Johnson and M. Frigo, "A modified split-radix FFT with fewer arithmetic operations," *IEEE Trans. Signal Process.*, vol. 55, no. 1, pp. 111–119, Jan. 2007.

Daniel J. F. Barros received the Licenciatura degree (hons) in electrical and electronics engineering from the University of Porto, Portugal, in 2004 and the M.S. degree in electrical engineering from Stanford University, Stanford, CA, in 2007, where he is currently working towards the Ph.D. degree in electrical engineering.

His research interests include single-mode optical-fiber communication, digital signal processing and RF circuits.

Joseph M. Kahn (M'90-SM'98-F'00) received the A.B., M.A. and Ph.D. degrees in physics from the University of California at Berkeley in 1981, 1983, and 1986, respectively.

From 1987–1990, he was at AT&T Bell Laboratories, Crawford Hill Laboratory, in Holmdel, NJ. He demonstrated multi-Gb/s coherent optical fiber transmission systems, setting world records for receiver sensitivity. From 1990–2003, he was on the faculty of the Department of Electrical Engineering and Computer Sciences at U.C. Berkeley, performing research on optical and wireless communications. Since 2003, he has been a Professor of Electrical Engineering at Stanford University, where he heads the Optical Communications Group. His current research interests include: rate-adaptive and spectrally efficient modulation and coding methods, coherent detection and associated digital signal processing algorithms, digital compensation of fiber nonlinearity, high-speed transmission in multimode fiber, and free-space systems. In 2000, he helped found StrataLight Communications (now Opnext Subsystems), where he served as Chief Scientist from 2000–2003.

Professor Kahn received the National Science Foundation Presidential Young Investigator Award in 1991. From 1993–2000, he served as a Technical Editor of *IEEE Personal Communications Magazine*. Since 2009, he has been an Associate Editor of IEEE/OSA JOURNAL OF OPTICAL COMMUNICATIONS AND NETWORKING.